

Fermi National Accelerator Laboratory

FERMILAB-Conf-97/180-E

CDF and DØ

Rapidity Gaps and Hard Diffraction at the Tevatron

Brad Abbott

For the CDF and DØ Collaborations

New York University

Fermi National Accelerator Laboratory

P.O. Box 500, Batavia, Illinois 60510

June 1997

Published Proceedings of *Les Rencontres de Physique de la Vallee D'Aoste*,
La Thuile, Italy, March 2-8, 1997

Disclaimer

This report was prepared as an account of work sponsored by an agency of the United States Government. Neither the United States Government nor any agency thereof, nor any of their employees, makes any warranty, expressed or implied, or assumes any legal liability or responsibility for the accuracy, completeness, or usefulness of any information, apparatus, product, or process disclosed, or represents that its use would not infringe privately owned rights. Reference herein to any specific commercial product, process, or service by trade name, trademark, manufacturer, or otherwise, does not necessarily constitute or imply its endorsement, recommendation, or favoring by the United States Government or any agency thereof. The views and opinions of authors expressed herein do not necessarily state or reflect those of the United States Government or any agency thereof.

Distribution

Approved for public release; further dissemination unlimited.

DOCONF-97-10

Conf-97/180-E

RAPIDITY GAPS AND HARD DIFFRACTION AT THE TEVATRON

Brad Abbott

*New York University
For the DØ and CDF Collaborations*

Abstract

Preliminary results on jet production with rapidity gaps in $p\bar{p}$ collisions are presented for both DØ and CDF. An excess of events with a forward rapidity gap is observed at both $\sqrt{s}=1800$ GeV and 630 GeV, consistent with a hard single diffractive process. The first evidence for diffractive W production is presented. A class of events with two forward gaps and central dijets is observed at $\sqrt{s}=1800$ GeV, a topology that is consistent with hard double pomeron exchange. Kinematic properties of events containing rapidity gaps are measured.

1 Introduction

The properties of elastic and diffractive scattering are well described in the context of Regge theory [1], [2] by pomeron exchange, where the pomeron is a color singlet with the quantum numbers of the vacuum [3], [4]. The exact nature of the pomeron, or whether it actually exists, is still an open question. Ingelman and Schlein's paper [5] proposed that the observation of jets in diffractive events would probe the partonic nature of the exchanged object(pomeron). They assumed that the pomeron can be treated as an object which exists within the proton, and therefore one can define a flux of pomerons within the proton and a pomeron structure function. They proposed a gluonic pomeron with either a hard structure $\sim \beta(1 - \beta)$ or a soft structure $(1 - \beta)^5$, where β is the momentum fraction of the parton with respect to the pomeron.

Hard diffraction studies, which involve the production of jets, has increased dramatically in recent years since the initial observation by UA8 [6]. These studies give new insights into the nature of the object being exchanged in such processes. An experimental signature for diffractive events is the presence of a rapidity gap, where a rapidity gap is defined as the lack of particle production above an energy threshold in a region of pseudorapidity, η . Usually dijets are produced via color exchange which results in particle production in the rapidity region between the jets and the beam. A rapidity gap arises due to the colorless nature of the pomeron, which causes the radiation to be suppressed in the event.

2 Hard Single Diffraction

In hard single diffraction a pomeron is emitted from one of the incident protons and interacts with a parton within the other proton. The pomeron carries less than 5% of the incident proton momentum, therefore the two jets are typically boosted and a rapidity gap is expected on the side opposite the jets. By tagging events with two forward jets, the fraction of events that are diffractive should be enhanced relative to standard QCD which has a symmetric jet η distribution.

For both DØ and CDF, events are selected by demanding at least two jets above an E_T threshold within an η region and requiring that both jets obey $\eta_1 \cdot \eta_2 > 0$. For DØ the E_T threshold is 12 GeV and both jets are required to have $1.6 < |\eta| < \sim 3.5$. For CDF the E_T threshold is 20 GeV and both jets are required to be within $1.8 < |\eta| < 3.5$. Since multiple $p\bar{p}$ interactions within the same beam crossing can destroy the rapidity gap, both

experiments demand only a single interaction. This leaves both experiments with a data sample of nearly 30,000 events at $\sqrt{s}=1.8$ TeV and DØ with approximately 12,000 events at $\sqrt{s}=630$ GeV.

DØ measures the number of electromagnetic calorimeter towers with energy > 200 MeV in the region $|\eta| > 1.6$ opposite the dijet system. Figure 1 shows the multiplicity distribution opposite the same side dijet system at DØ for $\sqrt{s}=1.8$ TeV. The large excess of events in the zero multiplicity bin is significantly greater than the expectation from multiplicity fluctuations and is consistent with a hard single diffractive process. By fitting the leading edge to a negative binomial distribution, the excess of events above the fit in the zero multiplicity bin is measured at $f_{DØ}=[0.67 \pm 0.05(\text{stat+sys on fit})]\%$.

CDF measures the fraction of jets produced by a hard single diffraction process by determining the correlation between the number of calorimeter towers with $E_T > 1.5$ GeV in the region $2.2 < |\eta| < 4.2$ and the occupancy of Beam-Beam counters (BBC) opposite the same side dijet system. The BBC are an array of 8 horizontal and 8 vertical scintillation counters placed perpendicular to the beam line covering the region $3.2 < |\eta| < 5.9$. An excess of events is found in the zero multiplicity bin consistent with a hard single diffractive process. The fraction of events due to a hard single diffractive process measured at CDF is $f_{CDF}=[0.75 \pm 0.05(\text{stat}) \pm 0.09(\text{sys})]\%$.

The presence of a hard single diffractive signal at $\sqrt{s}=630$ GeV has also been explored at DØ. Figure 2 shows the multiplicity distribution of electromagnetic towers opposite the same side dijet system at $\sqrt{s}=630$ GeV. A large excess of events is clearly seen above the negative binomial fit in the zero multiplicity bin. At this lower center of mass energy, the excess, which can be attributed to a hard single diffractive process, is measured to be between 1-2%.

3 Diffractive W Production

At the Tevatron, a hard-quark pomeron structure will result in measurable W diffractive production [7]. A hard-gluon pomeron can also produce diffractive W bosons, but at a rate lower by α_s and always with an associated jet. For diffractively produced $W^\pm \rightarrow e^\pm \nu$ events in which the pomeron is emitted by the proton, the rapidity gap is expected to be in the positive η direction (proton direction) and the e^\pm at negative η . This leads to an angle-gap correlation for diffractive W production. Additionally, since the pomeron is flavor symmetric and it is mainly valence quarks within the \bar{p} which participate in W production, one expects nearly twice as many electrons as positrons. This

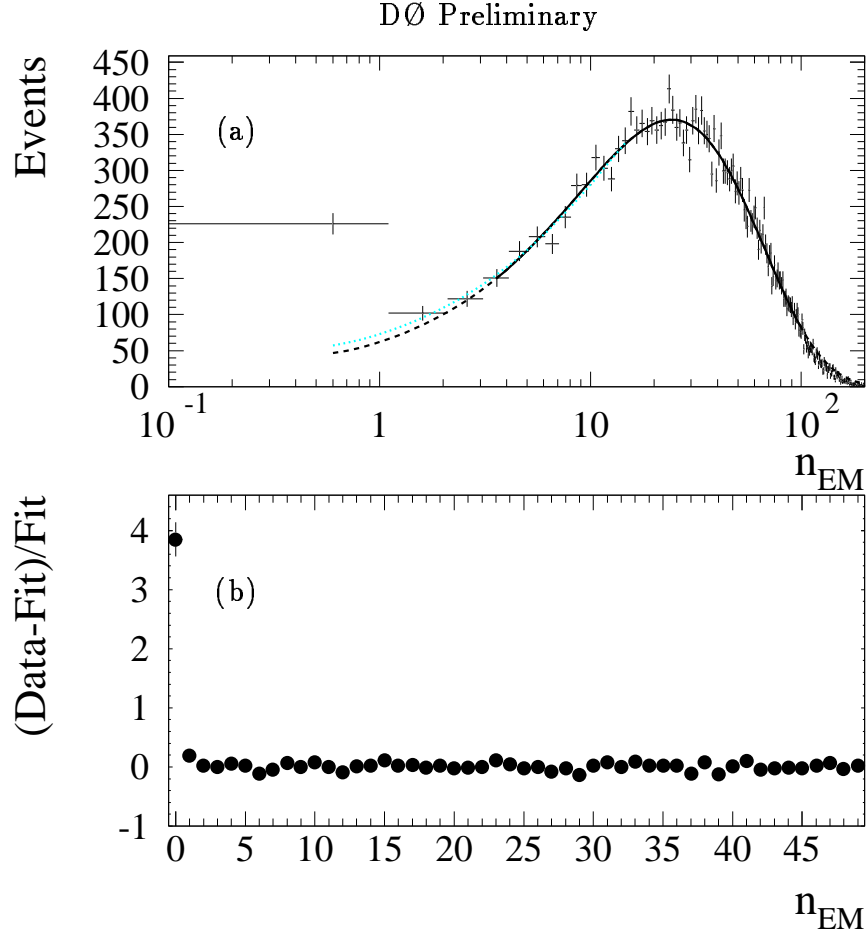


Figure 1: (a) The multiplicity distribution of electromagnetic calorimeter towers with energy greater than 200 MeV opposite the same side dijet system compared to two negative binomial fits at $\sqrt{s}=1800$ GeV. One fit is to the leading edge and the other fits to $n_{em}=100$. (b): Bin-by-bin fractional difference between data and the fit. The large excess of events in the zero multiplicity bin relative to the fit is consistent with a hard single diffractive process.

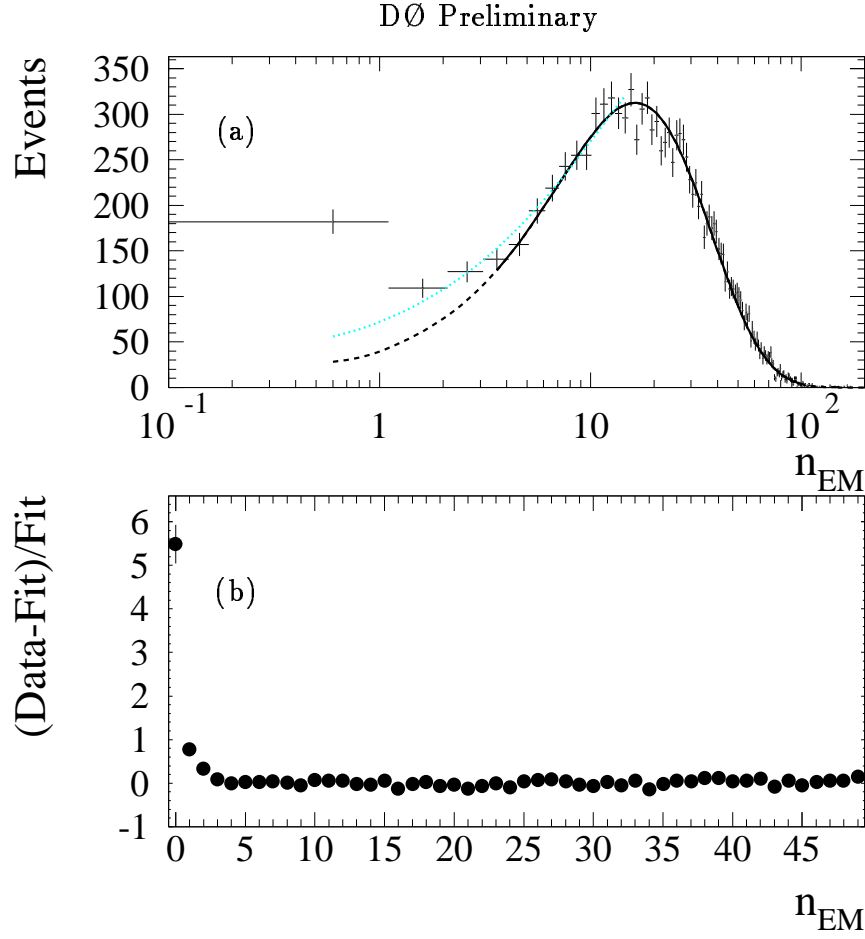


Figure 2: (a) The multiplicity distribution of electromagnetic calorimeter towers opposite the same side dijet system compared to two negative binomial fits at $\sqrt{s}=630$ GeV. One fit is to the leading edge and the other fits to $n_{em}=100$. (b) Bin-by-bin fractional difference between data and the fit. The large excess of events in the zero multiplicity bin relative to the fit is consistent with a hard single diffractive process.

leads to a charge-gap correlation. By measuring the correlations in W events, a signal can be extracted. The data sample was collected by the CDF experiment during both the 1992-1993 and the 1994-1995 runs of the collider. Events with missing $E_T > 20$ GeV and an isolated electron of $E_T > 20$ GeV with $|\eta| < 1.1$ were selected. After removing events with more than one primary vertex, 8246 events remained. The diffractively produced W signal is measured by analyzing the correlations between the η of the electron, η_e , or the sign of its charge, C_e , and the multiplicity of one or the other BBC. Each event enters into two different distributions. The first is a correlated distribution: $\eta_e \cdot \eta_{BBC} < 0$ (angle-correlated) or $C_e \cdot \eta_{BBC} > 0$ (charge-correlated) or $\eta_e \cdot C_e > 0$ and $\eta_e \cdot \eta_{BBC} < 0$ (doubly correlated). The second is an anti-correlated distribution $\eta_e \cdot \eta_{BBC} > 0$ (angle-anticorrelated) or $C_e \cdot \eta_{BBC} > 0$ (charge-anticorrelated) or $\eta_e \cdot C_e > 0$ and $\eta_e \cdot \eta_{BBC} > 0$ (doubly anticorrelated).

Figure 3 shows the observed correlations as a function of BBC multiplicity. The probability that the excess is consistent with non-diffractive production is 1.1×10^{-4} (3.8σ). From the excess of events in the zero multiplicity bin for the correlated variables, one finds the ratio of diffractively to non-diffractively produced W events to be $1.15\% \pm 0.55\%$.

The number of diffractive W events with an associated jet is relatively small. This small fraction of diffractive W +jet events implies that it is mostly quarks from the pomeron which participate in W production.

One can combine the results from the diffractive W production, which is sensitive to the quarks within the pomeron, and the diffractive jet production, which is sensitive to both the quarks and gluons within the pomeron. Both the CDF diffractive dijet and the diffractive W results are final and are corrected for the gap acceptance. This allows a measurement of the momentum fraction of the hard partons in the pomeron and the gluon fraction of hard partons in the pomeron. Figure 4 shows the allowed ranges when the W and jet data are combined by assuming a hard pomeron structure function $\beta G(\beta) \sim \beta(1-\beta)$. The pomeron gluon fraction is measured to be 0.7 ± 0.2 and the fraction of the total pomeron momentum carried by its hard partons is 0.18 ± 0.04 . The difference between the CDF and ZEUS measurement in the pomeron gluon fraction may be due to a discrepancy in the pomeron flux normalization [8].

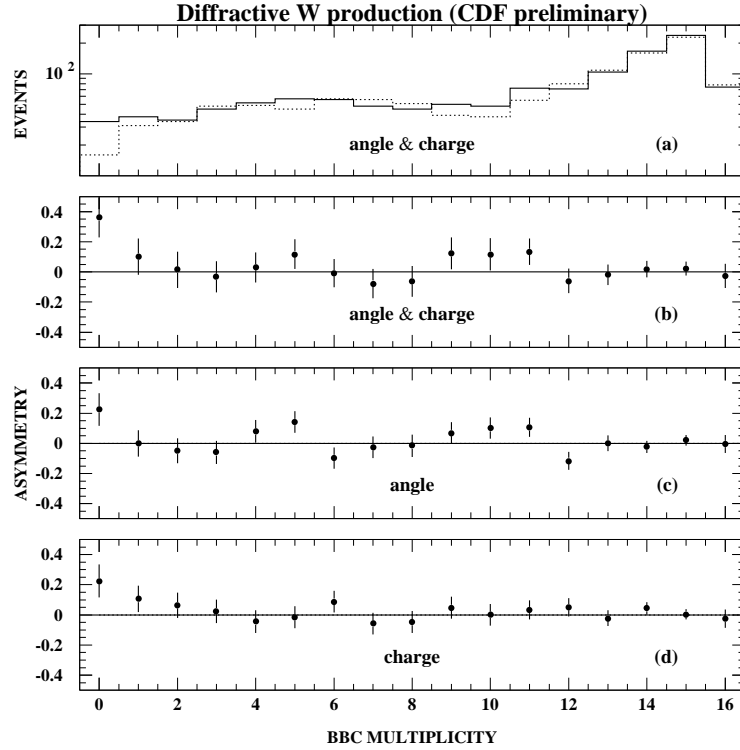


Figure 3: (a) Electron angle and charge doubly-correlated (solid) and anticorrelated (dashed) distributions versus BBC multiplicity, and (b) the corresponding asymmetry, defined as the bin-by-bin difference over the sum of the two distributions in (a). The diffractive signal is seen in the first bin as an excess of events in the correlated distribution in (a), and as a positive asymmetry in (b). An asymmetry is also seen in the first bin of the the individual angle (c) and charge (d) distributions.

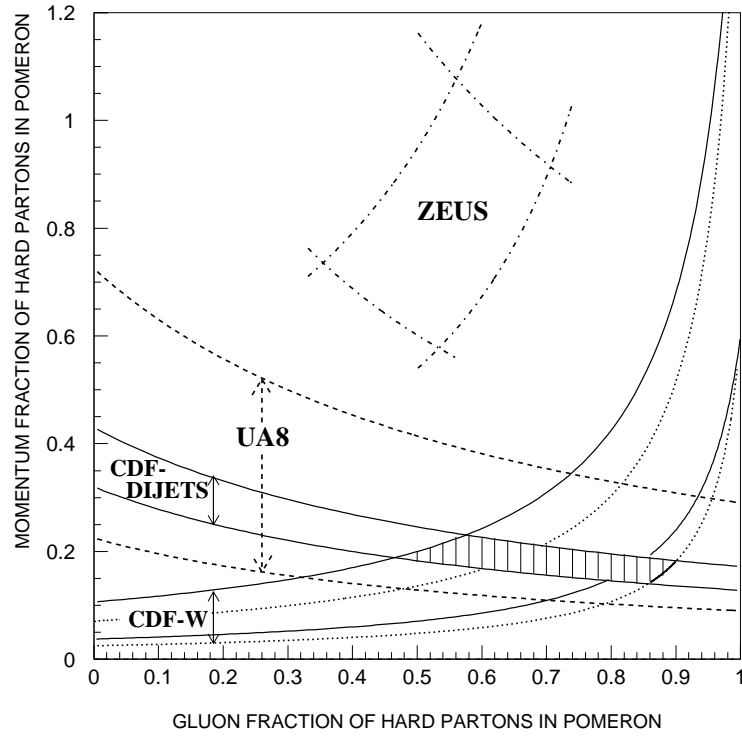


Figure 4: Momentum fraction versus gluon fraction of hard partons in the pomeron evaluated by comparing the measured diffractive rates with Monte Carlo predictions based on the standard pomeron flux and assuming that only hard pomeron partons participate in the diffractive processes. Results are shown for ZEUS (dashed-dotted), UA8(dashed) and the CDF dijet and W measurements. The CDF W result is shown for two(dotted) or three(solid) quark flavors in the pomeron.

4 Hard Double Pomeron

The hard single diffractive results show that approximately 1% of dijet events are produced diffractively. In hard double pomeron exchange, where pomerons from both the proton and the anti-proton interact, the signal is expected to be much smaller. Because the fraction of dijets produced from hard double pomeron exchange is expected to be small, both experiments have implemented a special trigger.

In order to enhance statistics for the hard double pomeron search, a single gap trigger has been implemented at DØ. This trigger is similar to an inclusive jet trigger with an additional demand that the number of level 0 hits on one side of the detector is zero. The level 0 counters are an array of scintillators used at DØ to tag inelastic scattering. By requiring that the number of electromagnetic calorimeter towers with energy greater than 200 MeV is zero and the number of level 0 hits is also zero on one side of the detector, the multiplicity of the other side of the detector can be measured. Figure 5 shows this multiplicity distribution. By fitting the distribution to a negative binomial, one sees an excess of events in the zero multiplicity bin. This excess of events are the hard double pomeron candidates and is found to be $\sim \mathcal{O}(10^{-6})$ of the inclusive dijet sample.

CDF has implemented a hard double pomeron trigger by using a roman pot on the west side of the detector which can measure a proton track with a Feynman x between 0.9 and 0.95. After demanding a track within the roman pot and two jets with $E_T > 7$ GeV in the central calorimeter, the multiplicity on the east side of the detector can be measured. Figure 6 shows the correlations between the multiplicities of the east calorimeter towers and the east BBC. An excess of events is clearly seen in the zero multiplicity bin showing evidence of events consistent with hard double pomeron exchange. The excess is measured to be $2.7 \pm 0.8 \times 10^{-6}$ of the inclusive dijet sample.

5 Rapidity Gaps Between Jets

The color singlet exchange signal has been previously established for events with centrally produced rapidity gaps [9],[10], [11]. The properties of the signal events are studied in finer detail to better understand the nature of the pomeron. In this analysis, the events have jets on opposite sides of the detector ($\eta_1 \cdot \eta_2 < 0$) and the multiplicity in the central η region is measured.

For CDF, two jets with $E_T > 20$ GeV and $1.8 < |\eta| < 3.5$ were required. Because multiple $p\bar{p}$ interactions can spoil the rapidity gap, only events with a single vertex were

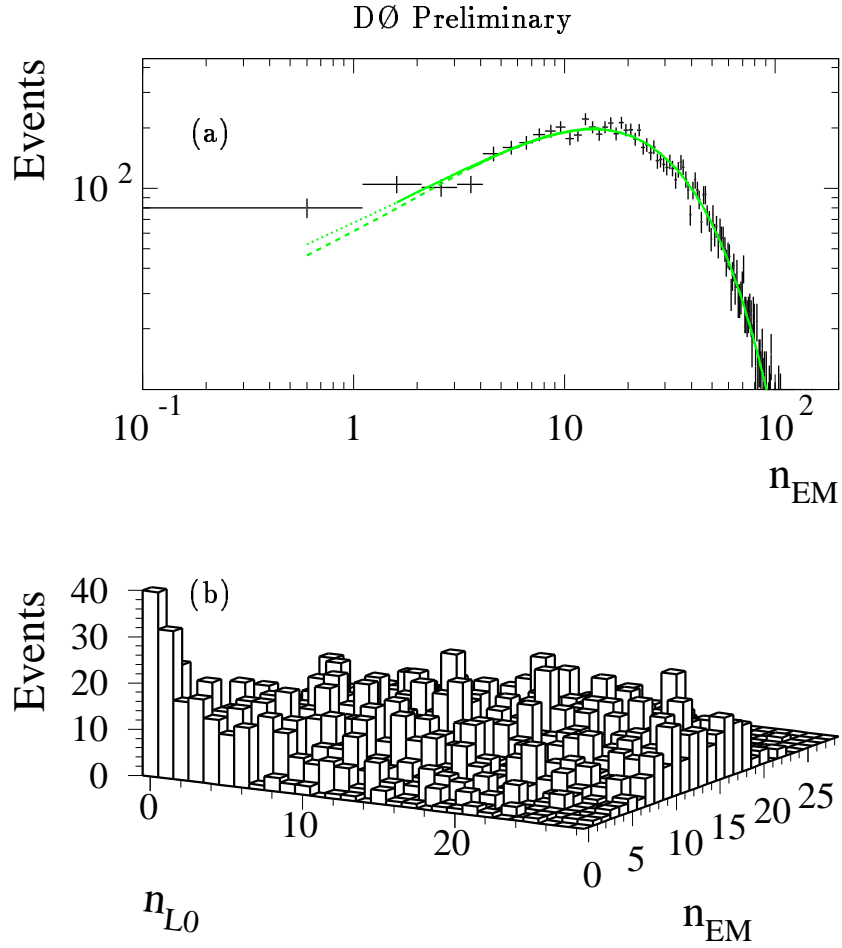


Figure 5: (a) The electromagnetic calorimeter multiplicity opposite the region requiring zero electromagnetic calorimeter towers and no level \emptyset hits. The excess of events in the zero multiplicity bin are the hard double pomeron exchange candidates. (b) Correlation between the number of level \emptyset hits and the number of electromagnetic calorimeter towers. A large excess is seen in the zero multiplicity bin for both detectors.

Forward East Multiplicities for Roman Pot Dijets

CDF Preliminary

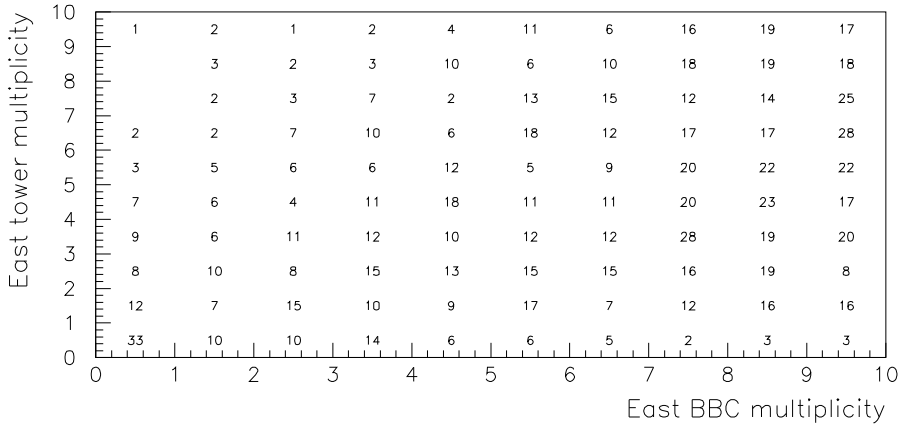
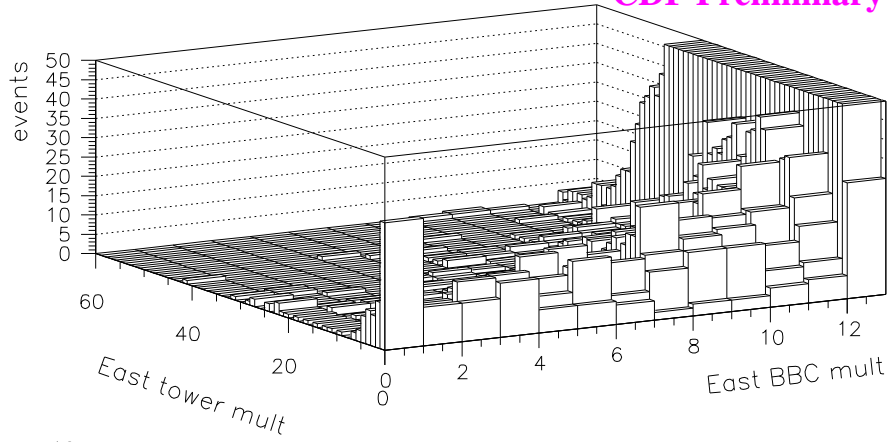


Figure 6: The east calorimeter tower multiplicity versus the east BBC multiplicity after requiring a roman pot track and two centrally produced jets. The excess of events in the zero multiplicity bin are the hard double pomeron exchange candidates.

examined. The correlations between the number of tracks with $P_T > 300$ MeV and the multiplicity of calorimeter towers with $E_T > 200$ MeV are studied. Events with same side jets ($\eta_1 \cdot \eta_2 > 0$) were analyzed to measure the background. Figure 7 shows the correlations between the number of calorimeter towers and the number of tracks in the region $|\eta| < 1.0$ for opposite side and same side dijet sample. The rapidity gap events in the opposite side sample are seen as a distinct peak in the bins with zero tracks and 0, 1, or 2 towers. No such peak is seen in the same side jet sample. The fraction of events with a central rapidity gap is measured to be $f_{CDF}=[1.13 \pm 0.12(\text{stat}) \pm 0.1(\text{sys})]\%$.

Figure 8 shows the E_T of jet 1 and jet 2 for both gap and background events from CDF. Also shown is the percent of events with a rapidity gap as a function of $\Delta\eta/2$.

DØ requires two jets with $E_T > 30$ GeV, $|\eta| > 1.6$ and $\Delta\eta > 4$. The fraction of events with a central rapidity gap is measured to be $f_{DØ}=[0.85 \pm 0.05(\text{stat}) \pm 0.07(\text{sys})]\%$

DØ has also started studying the \sqrt{s} dependence of the signal to better understand the nature of the pomeron. By comparing the fraction of events containing a rapidity gap at $\sqrt{s}=1.8$ TeV to $\sqrt{s}=630$ GeV, different x regions of the proton are probed giving different quark and gluon components. Therefore this ratio may be used to test for a different coupling of the color singlet to quarks or gluons. Events with two jets of $E_T > 12$ GeV and with $|\eta| > 1.9$ are selected. The n_{cal} multiplicity distributions for the two samples are shown in Fig. 9. The leading edge of each n_{cal} distribution is fitted using a single negative binomial distribution. The fraction of rapidity gap events is calculated from the excess of events over the fit in the first two bins divided by the total number of entries. It is found to be $0.6 \pm 0.1\%(\text{stat.})$ at $\sqrt{s} = 1800$ GeV and $1.6 \pm 0.2\%(\text{stat.})$ at $\sqrt{s} = 630$ GeV. The ratio R of the rapidity gap fractions at 630 and 1800 GeV is equal to $2.6 \pm 0.6\%(\text{stat.})$. The survival probability of the rapidity gap, defined as the probability of no spectator interactions, is expected to have only a logarithmic dependence on \sqrt{s} and therefore, can not account for the observed ratio of the rapidity gap fractions at the two center-of-mass energies.

6 Conclusion

Preliminary results are presented for many different diffractive processes. Both DØ and CDF find similar results for the fraction of diffractive events containing jets: $f_{CDF}=[0.75 \pm 0.05(\text{stat}) \pm 0.09(\text{sys})]\%$ and $f_{DØ}=[0.67 \pm 0.05(\text{stat+sys on fit})]\%$. Evidence of a hard single diffractive signal at $\sqrt{s}=630$ GeV is also found at DØ. The first evidence for diffractive W production is found at CDF. The fraction of W bosons which are diffractively

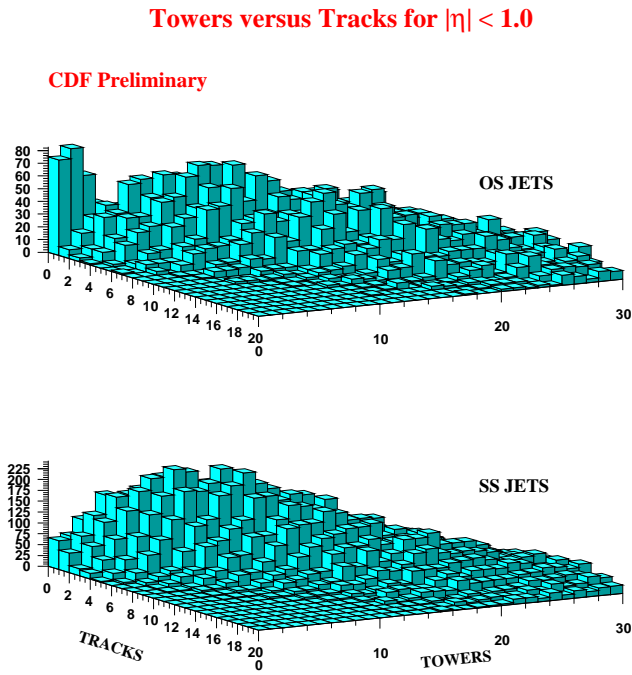


Figure 7: Tower versus track multiplicity distributions within $|\eta| < 1$ for the $N_{vertex}=1$ event samples of (a) opposite side jets and (b) same side jets. The peak in the bins with zero tracks and 0, 1 or 2 towers in (a) is attributed to rapidity gap events.

CDF Preliminary

Kinematic Comparison of Gap and Background Events

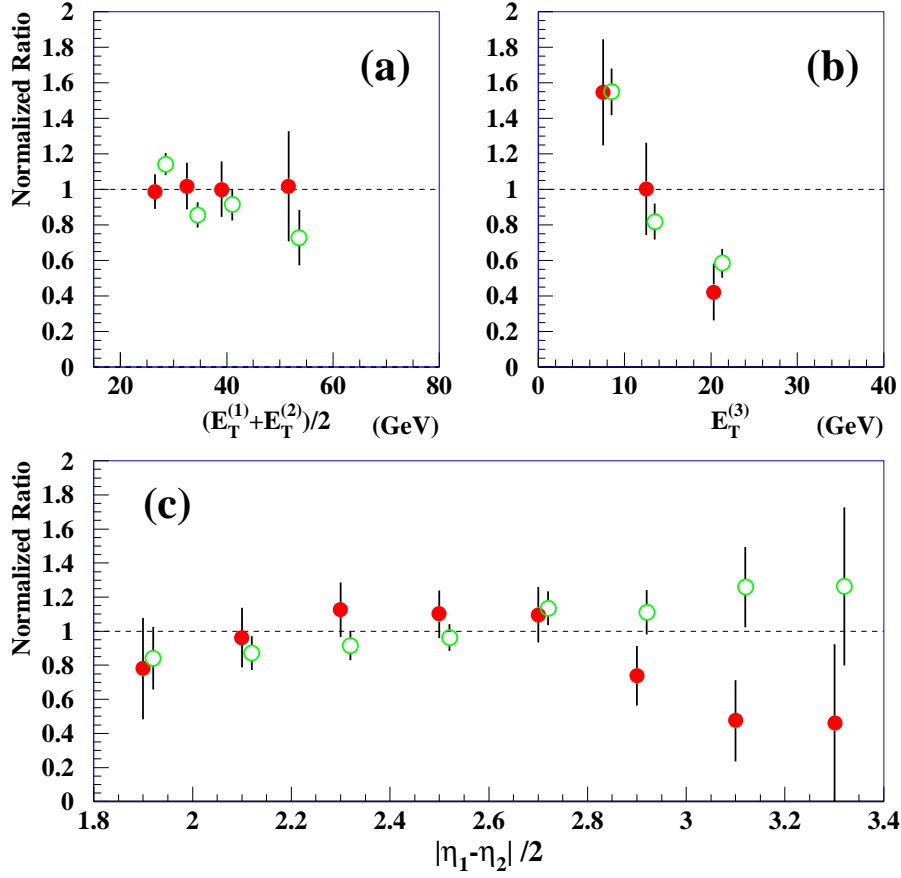


Figure 8: Comparison of distributions of (a) the average E_T of the two leading E_T jets for opposite-side rapidity gap events (solid) and same-side background events (open) and (b) the third jet E_T . Comparison of the normalized ratio (c) of the fraction of gap events as a function of $\Delta\eta/2$.

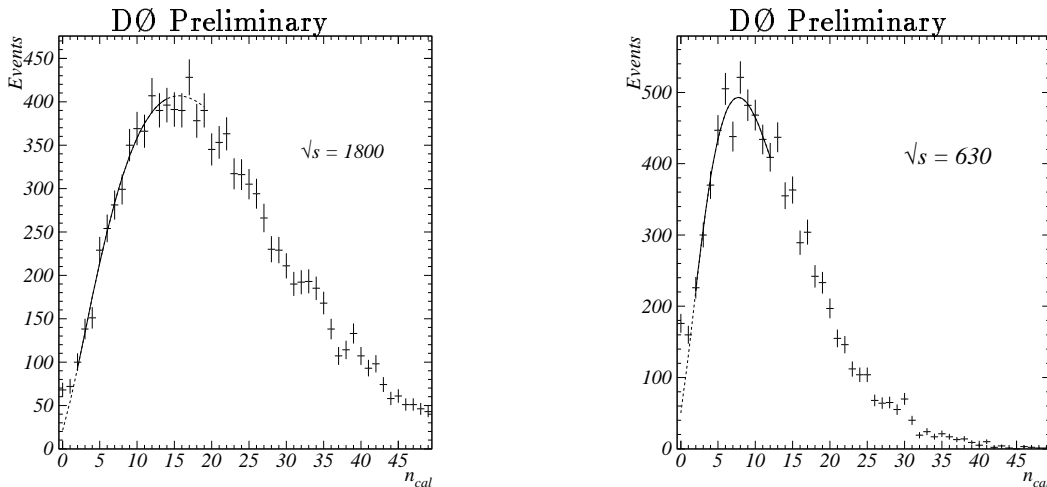


Figure 9: Central EM calorimeter multiplicities for the $\sqrt{s} = 1800$ GeV and 630 GeV samples. The negative binomial fits are also shown.

produced is measured to be $1.15\% \pm 0.55\%$. The small fraction of W +jet events implies that it is mainly quarks from the pomeron which participate in diffractive W production. By combining results from the diffractive W results and the diffractive jet results, the pomeron gluon fraction is measured to be 0.7 ± 0.2 and the fraction of the total pomeron momentum carried by its hard partons is 0.18 ± 0.04 . The first hard double pomeron search at the Tevatron has begun and double pomeron candidates have been observed at both CDF and DØ. Both experiments find similar results for the hard color singlet search: $f_{CDF}=[1.13 \pm 0.12(\text{stat}) \pm 0.1(\text{sys})]\%$ and $f_{DØ}=[0.85 \pm 0.05(\text{stat}) \pm 0.07(\text{fit})]\%$. CDF has presented final results on the E_T and η dependence of the color singlet signal. DØ is currently studying the E_T and η dependence of the color singlet signal, and has also been studying the \sqrt{s} dependence of the signal. The ratio of the rapidity gap fractions at $\sqrt{s}=630$ GeV and 1800 GeV is equal to $2.6 \pm 0.6\%(\text{stat})$.

We are grateful to the DØ and CDF Collaborations for discussions of their data.

References

- [1] T. Regge , Nuovo Cimento 14 (1959) 951.

- [2] P. D. B. Collins, An Introduction to Regge Theory and High Energy Physics, Cambridge University Press (1977)
- [3] K. Goulianos, Physics Reports **101** (1983) 169.
- [4] A. Donnachie and P.V. Landshoff, Nucl. Phys. **B244** (1984) 322; **B267** (1986) 690.
- [5] G. Ingelman and P. Schlein, Phys. Lett. **B152** (1985) 256.
- [6] UA8 Collaboration A. Brandt *et al.* Phys. Lett. B **297**, 417 (1992).
- [7] CDF Collaboration, F. Abe *et al.* Phys. Rev. Lett. **78** (1997) 2698
- [8] K. Goulianos, Phys. Lett. **B358** (1995) 379.
- [9] D0 Collaboration, S. Abachi *et al.* Phys. Rev. Lett. **72** (1994) 2332
- [10] CDF Collaboration, F. Abe *et al.* Phys. Rev. Lett. **74** (1995) 885
- [11] D0 Collaboration, S. Abachi *et al.* Phys. Rev. Lett. **76** (1996) 734